Organic–Inorganic Hybrids Based on Monovacant Keggin-type Silicotungstates and 3d–4f Heterometals

ARTICLE *in* CRYSTAL GROWTH & DESIGN · FEBRUARY 2012

Impact Factor: 4.89 · DOI: 10.1021/cg2012759

6 AUTHORS, INCLUDING:

Shaowei Zhang
Hunan University of Science and Technology
17 PUBLICATIONS **210** CITATIONS

CRYSTAL GROWTH & DESIGN

Article

pubs.acs.org/crystal

Organic–Inorganic Hybrids Based on Monovacant Keggin-type Silicotungstates and 3d-4f Heterometals

Shaowei Zhang, Junwei Zhao, Pengtao Ma, Huanni Chen, Jingyang Niu,* and Jingping Wang*

Institute of Molecular and Crystal Engineering, College of Chemistry and Chemical Engineering, Henan University Kaifeng, Henan 475004, P. R. China

Supporting Information

ABSTRACT: A series of organic–inorganic hybrid lacunary Keggin silicotungstate 3d-4f heterometallic derivatives, $\{[Cu(en)_2]_{1.5}Ln[(\alpha\text{-}SiW_{11}O_{39})_2]\}_2^{20-}$ [Ln = Gd^{III} for **1**, Tb^{III} for **2**, Dy^{III} for **3**, Er^{III} for **4**, Lu^{III} for **5**], $\{[Cu(en)_2]_{1.5}Ln[(\alpha\text{-}SiW_{11}O_{39})]\}^{2-}$ [Ln = La^{III} for **6**, Ce^{III}, for **7**] and $\{[Cu(en)_2(H_2O)][Cu(en)_2]_nLn[(\alpha\text{-}SiW_{11}O_{39})_2]\}^{m-}$ [(Ln, *n*, *m*) = (Pr^{III}, 2, 7) for **8**, (Sm^{III}, 3, 5) for **9**] (en = ethylenediamine) have been successfully synthesized under hydrothermal conditions and further characterized by elemental analyses, inductively coupled plasma atomic emission spectrometry (ICP-AES) analyses, X-ray powder diffraction (XRPD), IR spectra, thermogravimetric (TG) analyses, and single-crystal X-ray diffraction. The common features of **1**–**5** and **8**–**9** are that they all consist of a sandwich-type $[Ln(\alpha\text{-}SiW_{11}O_{39})_2]^{13-}$ polyoxoanion, whereas both **6** and **7** consist of the unusual 1:1 $[Ln(\alpha\text{-}SiW_{11}O_{39})]^{5-}$ units and $[Cu(en)_2]^{2+}$ coordination cations. **1**–**5** show dimeric structures, and **6**–**9** display unprecedented three-dimensional (3D) frameworks, representing the first 3D 3d-4f heterometallic silicotungstates. The features of **6** and **7** are that the components are closely packed along the 2_1 screw axis to generate scarce 5-connected network structures with the Schläfli symbol of $(4^8{\cdot}6^2)$, while **8** and **9** exhibit the 4-connected (6^6) topology and 6-connected $(4^8{\cdot}5^4{\cdot}6^3)$ topology structures, respectively. Furthermore, **2**, **3**, and **9** manifest apparent fluorescence signals, which can be assigned to the characteristic emissions of Tb^{III}, Dy^{III}, and Sm^{III} cations, respectively.

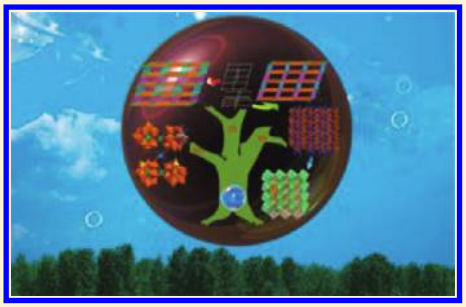

INTRODUCTION

The ongoing synthesis and exploitation for novel polyoxometalates (POMs) are predominantly driven by the structural diversities and potential applications in catalysis, photochemistry, electrochemistry, and magnetism.[1] Keggin POMs can act as early transition-metal oxide ligands, which can be functionalized by transition-metal (TM) or lanthanide (Ln) cations, resulting in TM-substituted POMs or Ln-substituted POMs. Hitherto, numerous TM-substituted Keggin POMs have been greatly studied.[2] Meanwhile, Ln-substituted Keggin-type POMs have been synthesized and structurally characterized resulting from the high coordination numbers and oxyphilic activities of the Ln cations, and their multiple physicochemical properties.[3] Though a few heterometallic 3d-4f POMs have been reported to date,[4] the investigation on the extended structures constructed by Keggin-type POMs and 3d-4f heterometals is very limited. Since the first 3d-4f heterometallic sandwiched Keggin-type POM was discovered by Müller et al. in 2007,[5] some 3d-4f heterometallic Keggin-type derivatives were prepared in succession, including a family of one-dimensional (1D) 3d-4f organic–inorganic hybrids $[\{Ln(PW_{11}O_{39})_2\}\{Cu_2(bpy)_2(\mu\text{-}ox)\}]^{9-}$ (Ln = La^{III}, Pr^{III}, Eu^{III}, Gd^{III}, Yb^{III}),[6] a trimeric $\{Fe^{III}\text{-}(\mu_3\text{-}O)_3\text{-}Ce^{III}\}$ heterometallic cluster substituted dilacunary Keggin arsenotungstate $[K\subset\{FeCe(AsW_{10}O_{38})(H_2O)_2\}_3]^{14-}$,[7] a heterometallic 3d-4f cluster related to the Weakley-type dimeric structure $[\{Ce(H_2O)_2\}_2Mn_2(B\text{-}\alpha\text{-}GeW_9O_{34})_2]^{8-}$,[8] a series of 1D chains constructed by $[Ln(PW_{11}O_{39})_2]^{11-}$ and $[Cu(en)_2]^{2+}$ groups.[9] In addition, a porous POM-based 4d-4f heterometals 3D framework $[\{Ag_3(H_2O)_2\}\ \{Ce_2(H_2O)_{12}\}H_5\subset\{H_2W_{11}Ce(H_2O)_4O_{39}\}_2]\cdot 8H_2O$ was also synthesized.[10]

However, to our knowledge, the reports on Keggin-type silicotungstates containing 3d-4f heterometals are very rare. Wang's group reported several heterometallic 3d-4f silicotungstates $[\{Ce(H_2O)_7\}_2Mn_4Si_2W_{18}O_{68}(H_2O)_2]^{6-}$,[11a] $\{Nd_2(H_2O)_{12}Cu_4(H_2O)_2(SiW_9O_{34})_2\}^{6-}$,[11b] and $[K_9Ln_6Fe_6(H_2O)_{12}(SiW_{10}O_{38})_6]^{26-}$ (Ln = Dy^{III}, Tb^{III}).[11c] In 2009, three unprecedented cubane-$\{LnCu_3(OH)_3O\}$ (Ln = La^{III}, Gd^{III}, Eu^{III}) substituted monovacant $[SiW_{11}O_{39}]^{8-}$ were isolated by Mialane et al.[12a] Meantime they also obtained a 1D double-chain derivative $[(\gamma\text{-}SiW_{10}O_{36})_2(Cr(OH)(H_2O))_3\ (La(H_2O)_7)_2]^{4-}$ by reaction of the trinuclear $[Cr_3(CH_3CO\ O)_7(OH)_2]$ and the divacant $[\gamma\text{-}SiW_{10}O_{36}]^{8}$.[12b] In recent years, our group has made great efforts in 3d-4f heterometallic POMs and isolated several types of 3d-4f POM derivatives: $\{[Cu(en)_2]_2[Na_2(H_2O)_{1.75}][K(H_2O)_3][Dy_2\ (H_2O)_2(GeW_{11}O_{39})_3]\}^{11-}$,[13a] $\{[Cu(en)_2]_2[Ce(\alpha\text{-}PW_{11}O_{39})_2]\}^{6-}$,[13b] $\{[Cu(dap)_2]_{4.5}[Dy(\alpha\text{-}PW_{11}O_{39})_2]\}^{2-}$,[13b] $\{[Cu(en)_2]_{1.5}[Cu\ (en)(2,2'\text{-bipy})(H_2O)_n]Ln[(\alpha\text{-}PW_{11}O_{39})_2]\}^{6-}$ [Ln = Ce^{III}, Pr^{III}],[13c] $\{[Cu(en)_2]_2(H_2O)[Cu(en)(2,2'\text{-bipy})]Ln[(\alpha\text{-}HPW_{11}O_{39})_2]\}^{4-}$ [Ln = Gd^{III}, Tb^{III}, Er^{III}],[13c] and

Received: September 26, 2011
Revised: November 10, 2011
Published: January 18, 2012

Table 1. Summary of Synthetic Conditions and Related Phases in the Preparation of 3d-4f Heterometallic Keggin-type POMs

major reactant	molar ratio of reactants	T [°C]	t [h]	phase
$As_2O_3/NaWO_4{\cdot}2H_2O/VOSO_4{\cdot}5H_2O/DyCl_3{\cdot}6H_2O/KCl/H_2O$	1/24.70/1.98/2.61/33.15/3019.76	70−80	3	$[((VO)_2Dy(H_2O)_4K_2(H_2O)_2Na(H_2O)_2)(\alpha\text{-B-}AsW_9O_{33})_2]^{8-S}$
$H_3PW_{12}O_{40}{\cdot}xH_2O/Ln^{3+}/CuCl_2{\cdot}2H_2O/CH_3COOK/2,2'\text{-bipy/oxalic/}H_2O$	1/0.14/1.93/29.14/1.93/1/20235.71	hot water	0.5	$[\{Ln(PW_{11}O_{39})_2\}\{Cu_2(bpy)_2(\mu\text{-ox})\}]^{9-6}$
$Na_2HAsO_4{\cdot}7H_2O/NaWO_4{\cdot}2H_2O/CeCl_3{\cdot}7H_2O/HMTA/FeCl_3{\cdot}6H_2O/HCl/H_2O$	1/10/2/1/2/18/2500	85−95	2	$[KC\{FeCe(AsW_{10}O_{38})(H_2O)_2\}_3]^{14-7}$
$K_{12}[Mn_4(H_2O)_2\}_2(B\text{-}\alpha\text{-}GeW_9O_{34})_2]/Ce(NH_4)_2(NO_3)_6/CsCl/H_2O$	1/2/10/22220	room temperature	a few weeks	$[\{Ce(H_2O)_2\}_2Mn_2(B\text{-}\alpha\text{-}GeW_9O_{34})_2]^{8-8}$
$Na_9[\alpha\text{-A-}PW_9O_{34}]{\cdot}7H_2O/CuCl_2{\cdot}2H_2O/Ce_2(SO_4)_3{\cdot}8H_2O/en/H_2O$	1/3.97/0.81/3.71/1392.51	120	120	$[\{Ce(PW_{11}O_{39})_2\}Cu(en)_2]^{9-9a}$
$H_3PW_{12}O_{40}{\cdot}xH_2O/Ln^{3+}/CuSO_4{\cdot}5H_2O/$ isophthalic acid/en/H_2O	1/5.56/16.67/5.33/16.67/7411.11	150	72	$\{[Cu(en)_2][Ln(PW_{11}O_{39})_2]\}^{9-9b}$
$K_4Na_6Mn[\{SiMn_2W_9O_{34}(H_2O)\}_2]{\cdot}33H_2O/Ce(SO_4)_2{\cdot}4H_2O/$potassiumitrate/$H_2O$	1/2/2/8335	boiling	2	$[\{Ce(H_2O)_7\}_2Mn_4Si_2W_{18}O_{68}(H_2O)_2]^{6-11a}$
$K_8[\gamma\text{-}SiW_{10}O_{36}]{\cdot}12H_2O/CuCl_2{\cdot}2H_2O/Nd(NO_3)_3/NaOH/AlCl_3/H_2O$	1/8.53/1.03/2.94/10.88/8170.59	boiling	5	$\{Nd_2(H_2O)_{12}Cu_4(H_2O)_2(SiW_9O_{34})_2\}^{6-11b}$
$K_8[\beta_2\text{-}SiW_{11}O_{39}]{\cdot}14H_2O/FeCl_3/NaCl/Dy_2O_3/en/H_2O$	1/4.77/3.92/10.31/11.54/4276.92	160	111.25	$[K_9Dy_6Fe_6(H_2O)_{12}(SiW_{10}O_{38})_6]^{26-11c}$
$K_8[\beta_2\text{-}SiW_{11}O_{39}]{\cdot}14H_2O/FeCl_3/NaCl/Tb_4O_7/en/H_2O$	1/4.77/3.92/5.15/5.77/4276.92	160	111.25	$[K_9Tb_6Fe_6(H_2O)_{12}(SiW_{10}O_{38})_6]^{26-11c}$
$Na_{10}[A\text{-}\alpha\text{-}SiW_9O_{34}]{\cdot}19H_2O/Cu(CH_3COO)_2/Ln^{3+}/en/H_2O$	1/3.50/1/3/2598.13	140	88	$\{LnCu_3(OH)_3O\}[SiW_{11}O_{39}]^{8-12a}$
$Cs_{10}[(\gamma\text{-}SiW_{10}O_{36})_2Cr(OH)(H_2O)_3]{\cdot}17H_2O/LaCl_3{\cdot}7H_2O/H_2O$	1/6/12966.67	80	2	$[(\gamma\text{-}SiW_{10}O_{36})_2(Cr(OH)(H_2O))_3(La(H_2O)_7)_2]^{4-12b}$
$\alpha\text{-}K_8[GeW_{11}O_{39}]{\cdot}nH_2O/DyCl_3/Cu(NO_3)_2{\cdot}3H_2O/en/H_2O$	1/0.62/3.45/2.27/1666.67	165	144	$\{[Cu(en)_2]_2[Na_2(H_2O)_{1.75}][K(H_2O)_3][Dy_2(H_2O)_2(GeW_{11}O_{39})_3]\}^{11-13a}$
$Na_9[A\text{-}\alpha\text{-}PW_9O_{34}]{\cdot}7H_2O/CuCl_2{\cdot}2H_2O/(NH_4)_2SO_4Ce(SO_4)_2/en/H_2O$	1/3.98/0.86/3.76/1396.98	160	216	$[Cu(en)_2]_2H_6[Ce(\alpha\text{-}PW_{11}O_{39})_2]{\cdot}8H_2O^{13b}$
$Na_9[A\text{-}\alpha\text{-}PW_9O_{34}]{\cdot}7H_2O/CuCl_2{\cdot}2H_2O/DyCl_3/dap/H_2O$	1/3.85/1.63/6.03/2895.83	160	216	$[Cu(dap)_2(H_2O)][Cu(dap)_2]_{4.5}[Dy(\alpha\text{-}PW_{11}O_{39})_2]{\cdot}4H_2O^{13b}$
$[\alpha\text{-}PW_9O_{34}]^{9-}/[\alpha\text{-}PW_{11}O_{39}]^{7-}/LnCl_3/CuCl_2{\cdot}2H_2O/en/2,2'\text{-bipy/}H_2O$	1/0.94/1.5/3.28/8.22/1.44/3088.89	170	96	$\{[Cu(en)_2]_{1.5}[Cu(en)(2,2'\text{-bipy})(H_2O)_n]Ln[(\alpha\text{-}PW_{11}O_{39})_2]\}^{6-13c}$

$\{[Cu(en)_2]_{1.5}[Cu(en)\ (2,2'\text{-bipy})]Nd[(\alpha\text{-}H_5PW_{11}O_{39})_2]\}^{3-}$.[13c] Very recently, we have expanded our research to 3d-4f heterometallic silicotungstate derivatives by reaction of $K_4[\alpha\text{-}SiW_{12}O_{40}]{\cdot}17H_2O$, Ln^{III} cations, Cu^{II} cations, and en to expect organic−inorganic hybrid high-dimensional 3d-4f silicotungstate derivatives based on the following considerations: (i) Most of the previously reported 3d-4f substituted Keggin-type POMs were synthesized by reaction of lacunary Keggin-type POM derivatives with 3d-4f heterometals (Table 1). As is known, the saturated Keggin-type $[SiW_{12}O_{40}]^{4-}$ POMs readily degrade and transform into monovacant, divacant, trivacant, even tetravacant Keggin derivatives and can also isomerize to the α-, β-, or γ-framework (Scheme 1), such as $[\alpha\text{-}SiW_{11}\ O_{39}]^{8-}$, $[\beta_2\text{-}SiW_{11}O_{39}]^{8-}$, $[\gamma\text{-}SiW_{10}O_{36}]^{8-}$, $[\alpha\text{-}SiW_9O_{34}]^{10-}$, $[\beta\text{-}SiW_9O_{34}]^{10-}$, $[\beta\text{-}SiW_8O_{31}]^{10-}$, and $[\gamma\text{-}SiW_8O_{31}]^{10-}$, resulting in the possibility for the structural variety of novel POM derivatives.[12a,14,15] (ii) In contrast to other 3d TM caions, Cu^{II} cations present more flexible coordination modes (square, trigonal bipyramid, square pyramid, and octahedron) than the other TM cations; the presence of the Jahn−Teller effect of the octahedron and pseudo-Jahn−Teller effect of the square pyramid for Cu^{II} cations can form different linkage modes to overcome steric hindrance, leading to novel structures.[13c,16] As a result, Cu^{II} cations can be the good candidates as 3d TM cation sources. (iii) In addition, some current efforts indicate that some organic N-ligands can act as good donors to coordinate to electrophilic TM cations, readily generating TM complexes, which can work as the bridges to form high-dimensional structures.[13c,15] Thus, the use of the aliphatic diamine ligand en was fully considered during our preparation of novel 3d-4f-heterometal-containing POMs. On the basis of the above considerations, a family of organic−inorganic hybrid 3d-4f-heterometal-containing Keggin silicotungstate derivatives, $\{[Cu(en)_2]_{1.5}Ln[(\alpha\text{-}SiW_{11}O_{39})_2]\}_2^{20-}$ [Ln = Gd^{III} for **1**, Tb^{III} for **2**, Dy^{III} for **3**, Er^{III} for **4**, Lu^{III} for **5**], $\{[Cu\ (en)_2]_{1.5}Ln[(\alpha\text{-}Si W_{11}O_{39})]\}^{2-}$ [Ln = La^{III} for **6**, Ce^{III}, for **7**], and $\{[Cu(en)_2(H_2O)][Cu(en)_2]_nLn[(\alpha\text{-}SiW_{11}O_{39})_2]\}^{m-}$ [(Ln, n, m) = (Pr^{III}, 2, 7) for **8**, (Sm^{III}, 3, 5) for **9**] have been successfully obtained under hydrothermal conditions. The common features of **1**−**5** and **8**−**9** are that they all consist of a sandwich-type $[Ln(\alpha\text{-}SiW_{11}O_{39})_2]^{13-}$ POMs, whereas both **6** and **7** consist of the unusual 1:1 $[Ln(\alpha\text{-}SiW_{11}O_{39})]^{5-}$ POMs as the fundamental building blocks and $[Cu(en)_2]^{2+}$ coordination cations as bridged-cations. **1**−**5** show the dimeric structures, **6**−**9** exhibit the unprecedented 3D frameworks, representing the first 3D 3d-4f heterometallic silicotungstates. The features of **6** and **7** are that the components are closely packed along the 2_1 screw axis to produce scarce 5-connected network structures with the Schläfli symbol of $(4^8{\cdot}6^2)$, while **8** and **9** display the 4-connected (6^6) topology and 6-connected $(4^8{\cdot}5^4{\cdot}6^3)$ topology structures, respectively. Furthermore, the luminescent properties of **2**, **3**, and **9** have been examined.

EXPERIMENTAL SECTION

General Methods and Materials. $K_4[\alpha\text{-}SiW_{12}\ O_{40}]{\cdot}17H_2O$ was prepared as described in the literature[17] and confirmed by IR spectra. Other chemical reagents were purchased without further purification. Elemental analyses (C, H, and N) were conducted on a Perkin-Elmer 2400-II CHNS/O analyzer. Inductively coupled plasma (ICP) analyses were performed on a Perkin-Elmer Optima2000 ICP-OES spectrometer. IR spectra were obtained from a solid sample palletized with KBr pellets on a Nicolet FT-IR 360 spectrometer in 4000−400 cm^{-1}. X-ray powder diffraction (XRPD) were performed on a Philips X'Pert-MPD instrument with Cu Kα radiation (λ = 1.54056 Å) in the range 2θ = 10−40° at 293 K. Thermogravimetric (TG) analyses were performed under N_2 atmosphere on a Mettler-Toledo TGA/SDTA851^e instrument

dx.doi.org/10.1021/cg2012759 | Cryst. Growth Des. 2012, 12, 1263−1272

Scheme 1. Transformations among Different Keggin-type Silicotungstate Derivatives

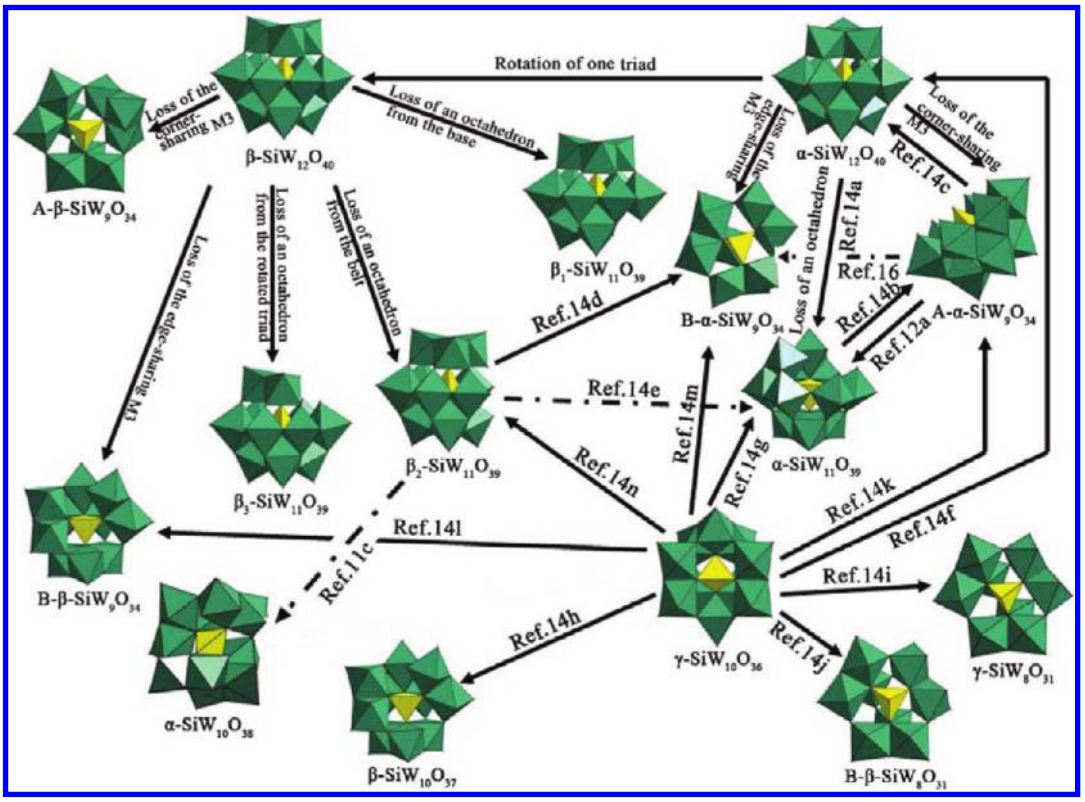

with a heating rate of 10 °C·min^{-1} from 25 to 800 °C. Photolumenescence measurements were performed on an F-7000 fluorescence spectrophotometer.

Syntheses of $K(enH_2)_4[Cu(en)_2(H_2O)]_2\{[Cu(en)_2]_{1.5}Gd[(\alpha\text{-}H_{1.75}SiW_{11}O_{39})_2]\}_2\cdot\sim15H_2O$ (1). $K_4[\alpha\text{-}SiW_{12}O_{40}]\cdot17H_2O$ (0.50 g, 0.15 mmol), $GdCl_3\cdot6H_2O$ (0.10 g, 0.27 mmol), $CuCl_2\cdot2H_2O$ (0.10 g, 0.59 mmol), and en (0.10 mL, 1.48 mmol) were successively dissolved in water (10 mL). After being stirred for 3 h, the resulting mixture was sealed in a 30 mL Telfon-lined stainless steel autoclave, kept at 170 °C for 5 days, and then slowly cooled to room temperature. Purple block crystals were collected by filtering, washed with distilled water, and dried in air. Yield: ca. 0.18 g, 0.014 mmol, 37% (based on $K_4[\alpha\text{-}SiW_{12}O_{40}]\cdot17H_2O$). Anal. Calcd. (%) for **1**: C 2.68, H 1.30, N 3.13, Cu 2.54, Gd 2.51, K 0.31, Si 0.90, W 64.55. Found: C 2.79, H 1.42, N 3.25, Cu 2.69, Gd 2.74, K 0.41, Si 1.03, W 64.36. IR (KBr pellets): 3433 (w), 3309 (w), 3233(w), 3141(sh), 1630 (w), 1582 (m), 1449 (m), 1392 (m), 1276 (w), 1102 (w), 1041 (m), 1006 (m), 946 (s), 887 (s), 831 (m), 770 (s), 724 (s) cm^{-1}.

Synthesis of $K(enH_2)_4[Cu(en)_2(H_2O)]_2\{[Cu(en)_2]_{1.5}Tb[(\alpha\text{-}H_{1.75}SiW_{11}O_{39})_2]\}_2\cdot\sim15H_2O$ (2). The preparation of **2** was similar to **1**, except that $TbCl_3\cdot6H_2O$ (0.10 g, 0.27 mmol) replaced $GdCl_3\cdot6H_2O$. Yield: 0.21 g, 0.017 mmol, 45% (based on $K_4[\alpha\text{-}SiW_{12}O_{40}]\cdot17H_2O$). Anal. Calcd. (%) for **2**: C 2.68, H 1.29, N 3.13, Cu 2.53, Tb 2.54, K 0.31, Si 0.90, W 64.53. Found: C 2.81, H 1.44, N 3.27, Cu 2.67, Tb 2.68, K 0.43, Si 1.02, W 64.35. IR (KBr pellets): 3441 (w), 3312 (w), 3229(w), 3145(sh), 1622 (w), 1585 (m), 1457 (m), 1397 (m), 1276 (w), 1101 (w), 1042 (m), 1005 (m), 943 (s), 889 (s), 824 (m), 767 (s), 722 (s) cm^{-1}.

Synthesis of $K(enH_2)_6[Cu(en)_2(H_2O)]_2\{[Cu(en)_2]_{1.5}Dy[(\alpha\text{-}H_{0.75}SiW_{11}O_{39})_2]\}_2\cdot\sim10H_2O$ (3). The preparation of **3** was similar to **1**, except that $DyCl_3\cdot6H_2O$ (0.10 g, 0.27 mmol) replaced $GdCl_3\cdot6H_2O$. Yield: 0.18 g, 0.014 mmol, 38% (based on $K_4[\alpha\text{-}SiW_{12}O_{40}]\cdot17H_2O$). Anal. Calcd. (%) for **3**: C 3.06, H 1.34, N 3.57, Cu 2.53, Dy 2.59, K 0.31, Si 0.89, W 64.34. Found: C 3.15, H 1.49, N 3.66, Cu 2.38, Dy 2.74, K 0.42, Si 1.05, W 64.13. IR (KBr pellets): 3440 (w), 3308 (w), 3230(w), 3142(sh), 1617 (w), 1585 (m), 1455(m), 1385 (m), 1280 (w), 1099 (w), 1042 (m), 1005 (m), 946 (s), 890 (s), 823 (m), 770 (s), 722 (s) cm^{-1}.

Synthesis of $K(enH_2)_4[Cu(en)_2(H_2O)]_2\{[Cu(en)_2]_{1.5}Er[(\alpha\text{-}H_{1.75}SiW_{11}O_{39})_2]\}_2\cdot\sim15H_2O$ (4). The preparation of **4** was similar to **1**, except that $ErCl_3\cdot6H_2O$ (0.10 g, 0.27 mmol) replaced $GdCl_3\cdot6H_2O$. Yield: 0.17 g, 0.014 mmol, 36% (based on $K_4[\alpha\text{-}SiW_{12}O_{40}]\cdot17H_2O$). Anal. Calcd. (%) for **4**: C 2.68, H 1.29, N 3.12, Cu 2.53, Er 2.67, K 0.31, Si 0.90, W 64.45. Found: C 2.81, H 1.41, N 3.21, Cu 2.67, Er 2.85, K 0.19, Si 0.76, W 64.28. IR (KBr pellets): 3428 (w), 3301 (w), 3235(w), 3140(sh), 1627 (w), 1587 (m), 1455 (m), 1395 (m), 1275 (w), 1098 (w), 1042 (m), 1007 (m), 941 (s), 889 (s), 828 (m), 768 (s), 720 (s) cm^{-1}.

Synthesis of $K(enH_2)_4[Cu(en)_2(H_2O)]_2\{[Cu(en)_2]_{1.5}Lu[(\alpha\text{-}H_{1.75}SiW_{11}O_{39})_2]\}_2\cdot\sim15H_2O$ (5). The preparation of **5** was similar to **1**, except that $LuCl_3\cdot6H_2O$ (0.10 g, 0.26 mmol) replaced $GdCl_3\cdot6H_2O$. Yield: 0.20 g, 0.016 mmol, 42% (based on $K_4[\alpha\text{-}SiW_{12}O_{40}]\cdot17H_2O$). Anal. Calcd. (%) for **5**: C 2.68, H 1.29, N 3.12, Cu 2.53, Lu 2.78, K 0.31, Si 0.89, W 64.37. Found: C 2.79, H 1.42, N 3.26, Cu 2.34, Lu 2.65, K 0.43, Si 1.04, W 64.52. IR (KBr pellets): 3438 (w), 3304 (w), 3264(w), 3145(sh), 1622 (w), 1586 (m), 1456 (m), 1395 (m), 1277 (w), 1098 (w), 1041 (m), 991 (m), 942 (s), 891 (s), 828 (m), 768 (s), 722 (s) cm^{-1}.

Synthesis of $(enH_2)_{0.5}\{[Cu(en)_2]_{1.5}La[(\alpha\text{-}HSiW_{11}O_{39})]\}\cdot\sim3H_2O$ (6). The preparation of **6** was similar to **1**, except that $LaCl_3\cdot6H_2O$ (0.10 g, 0.27 mmol) replaced $GdCl_3\cdot6H_2O$. Yield: 0.13 g, 0.041 mmol, 27% (based on $K_4[\alpha\text{-}SiW_{12}O_{40}]\cdot17H_2O$). Anal. Calcd. (%) for **6**: C 2.65, H 1.14, N 3.09, Cu 3.00, La 4.38, Si 0.88, W 63.69. Found: C 2.77, H 1.29, N 3.25, Cu 2.87, La 4.55, Si 1.06, W 63.48. IR (KBr pellets): 3430 (w), 3307 (w), 3245(w), 3130(sh), 1614 (w), 1584 (m), 1446 (m), 1384 (m), 1273 (w), 1105 (w), 1035 (m), 1001 (m), 978 (s), 951 (s), 901 (s), 821 (m), 775 (s), 702 (s) cm^{-1}.

Synthesis of $(enH_2)_{0.5}\{[Cu(en)_2]_{1.5}Ce[(\alpha\text{-}HSiW_{11}O_{39})]\}\cdot\sim2H_2O$ (7). The preparation of **7** was similar to **1**, except that $CeCl_3\cdot6H_2O$ (0.10 g, 0.27 mmol) replaced $GdCl_3\cdot6H_2O$. Yield: 0.11 g, 0.036 mmol, 24% (based on $K_4[\alpha\text{-}SiW_{12}O_{40}]\cdot17H_2O$). Anal. Calcd. (%) for **7**: C 2.66, H 1.09, N 3.10, Cu 3.02, Ce 4.44, Si 0.89, W 64.03. Found: C 2.79, H 1.18, N 3.24, Cu 3.19, Ce 4.57, Si 1.01, W 63.86. IR (KBr pellets): 3449 (w), 3308 (w), 3248(w), 3137(sh), 1603 (w), 1582 (m), 1448 (m), 1385 (m), 1275 (w), 1096 (w), 1036 (m), 1002 (m), 978 (s), 948 (s), 899 (s), 820 (m), 773 (s), 703 (s) cm^{-1}.

Synthesis of $(enH_2)_2\{[Cu(en)_2(H_2O)][Cu(en)_2]_2Pr[(\alpha\text{-}H_{1.5}SiW_{11}O_{39})_2]\}\cdot\sim6H_2O$ (8). The preparation of **8** was similar to **1**, except that $PrCl_3\cdot6H_2O$ (0.10 g, 0.27 mmol) replaced $GdCl_3\cdot6H_2O$. Yield: 0.17 g, 0.026 mmol, 35% (based on $K_4[\alpha\text{-}SiW_{12}O_{40}]\cdot17H_2O$).

dx.doi.org/10.1021/cg2012759 | Cryst. Growth Des. 2012, 12, 1263–1272

Anal. Calcd. (%) for **8**: C 3.05, H 1.36, N 3.56, Cu 3.03, Pr 2.24, Si 0.89, W 64.26. Found: C 3.17, H 1.24, N 3.68, Cu 2.88, Pr 2.47, Si 1.06, W 64.08. IR (KBr pellets): 3435 (w), 3302 (w), 3244(w), 3140(sh), 1617 (w), 1588 (m), 1455 (m), 1395 (m), 1279 (w), 1098 (w), 1046 (m), 1001 (m), 943 (s), 886 (s), 821 (m), 763 (s), 719 (s) cm^{-1}.

Synthesis of $(enH_2)\{[Cu(en)_2(H_2O)][Cu(Hen)_2][Cu(en)_2]_2$ Sm-$[(\alpha\text{-}H_{0.5}SiW_{11}O_{39})_2]\}\cdot\sim 6H_2O$ (9). The preparation of **9** was similar to **1**, except that $SmCl_3\cdot 6H_2O$ (0.10 g, 0.27 mmol) replaced $GdCl_3\cdot 6H_2O$. Yield: 0.15 g, 0.024 mmol, 32% (based on $K_4[\alpha\text{-}SiW_{12}O_{40}]\cdot 17H_2O$). Anal. Calcd. (%) for **9**: C 3.36, H 1.43, N 3.92, Cu 3.96, Sm 2.34, Si 0.87, W 62.95. Found: C 3.17, H 1.58, N 3.76, Cu 3.79, Sm 2.55, Si 1.02, W 63.29. IR (KBr pellets): 3436 (w), 3289 (w), 3253(w), 3140(sh), 1620 (w), 1590 (m), 1459 (m), 1384 (m), 1279 (w), 1105 (w), 1046 (m), 1006 (m), 940 (s), 889 (s), 826 (m), 769 (s), 721 (s) cm^{-1}.

X-ray Crystallography. Intensity data for **1**−**9** were collected on Bruker Apex-II CCD diffractometer with Mo Kα monochromated radiation (λ = 0.71073 Å) at 296(2) K. Routine Lorentz polarization and empirical absorption corrections were applied. The structures were solved by direct methods and refined by full-matrix least-squares methods on F^2 with the SHELXTL-97 program package.[18] No hydrogen atoms associated with the water molecules were located from the difference Fourier map. Positions of the hydrogen atoms attached to the carbon and nitrogen atoms were geometrically placed. All hydrogen atoms were refined isotropically as a riding mode using the default SHELXTL parameters. A summary of crystallographic data and structural refinements for **1**−**9** are summarized in Table 2. CCDC reference nos. 833559−833567 for **1**−**9**, respectively. These data can be obtained free of charge from The Cambridge Crystallographic Data Centre via www. ccdc. cam.ac.uk/data_ request/cif.

RESULTS AND DISCUSSION

Synthesis. Though 3d-4f heterometallic POMs exhibit interesting structures and fascinating properties make them become candidates for luminescent materials and magnetic materials,[4−13] the reports on 3d-4f heterometallic POMs remain very limited, especially for Keggin silicotungstates, which provide us a good opportunity to explore the domain with the aim to discover multidimensional structures with interesting properties. As is well-known, the oxyphilic Ln cations are easily bound to the surface oxygen atoms of the highly negative lacunary POMs, usually resulting in immediate precipitation rather than crystallization.[4b,19] Because the reactions between POMs and TM cations are less active, when Ln and TM cations simultaneously react with POMs, the reaction competition will unavoidably exist among the strongly oxyphilic Ln cations and relatively less active TM ions in the reaction system.[7,11] However, we find that it is more difficult to control the syntheses of 3d-4f heterometallic POMs with organic ligands under conventional aqueous solution methods, which is mainly due to the fact that the organic ligands always have very poor solubility in aqueous solutions. We choose the hydrothermal method to exploit this system because it has been proven to be an effective method in synthesizing organic−inorganic hybrid POMs.[13c,15] On one hand, because solubilities of materials increase under hydrothermal conditions, which can enhance the opportunity of the reaction among different reactants, a variety of inorganic and organic components could be introduced. On the other hand, the reduced viscosity of water under hydrothermal conditions increases the diffusion processes; therefore, it would be possible to harvest good quality crystals because the solvent extraction of solids and crystal growth from solution are favorable.[13c,15] Moreover, hydrothermal conditions are easy to make the reaction shift from the thermodynamic to the kinetic; as a result, the equilibrium phases are replaced by structurally more complicated metastable phases, and the metastable kinetic POM phases or intermediate phases rather than thermodynamic phases are more easily captured.[13c,15] Recently, by using this approach, we successfully obtained a series of novel 3d-4f heterometallic silicotungstate POMs **1**−**9**. Initially, **1** was isolated by reaction of $K_4[\alpha\text{-}SiW_{12}O_{40}]\cdot 17H_2O$, $GdCl_3\cdot 6H_2O$, and $CuCl_2\cdot 2H_2O$ in the presence of en at 170 °C. To investigate the influence of different TM cations on structural diversity, when the Cr^{III}, Mn^{II}, Fe^{II}, Co^{II}, Ni^{II}, Zn^{II}, or Cd^{II} cations replaced the Cu^{II} cation under the same conditions, unfortunately, only some amorphous precipitates were discovered, indicating that the TM cations may play a major factor in constructing 3d-4f heterometallic POMs. In addition, experimental results show that increasing or decreasing the amount of $GdCl_3\cdot 6H_2O$ is unfavorable to yield the products, suggesting that the amount of $GdCl_3\cdot 6H_2O$ also plays a key role in generating the products. Notably, during the course of our exploration, considering the effect of lanthanide contraction on structural diversity (Scheme 2), when replacing the Gd^{III} cation with Tb^{III}, Dy^{III}, Er^{III}, or Lu^{III} cations under the same conditions, interestingly, analogous structures **2**−**5** were obtained. When $LaCl_3\cdot 6H_2O$ or $CeCl_3\cdot 6H_2O$ replaced $GdCl_3\cdot 6H_2O$, 3D structures **6** and **7** were harvested, which consist of the unusual 1:1 $[Ln(\alpha\text{-}SiW_{11}O_{39})]^{5-}$ POMs and $[Cu(en)_2]^{2+}$ coordination cations. Under similar conditions, when Pr^{III} or Sm^{III} cations were employed, unexpectedly, two other types of 3D framework structures **8** and **9** were presented, representing the first 3D 3d-4f heterometallic silicotungstates with the Schläfli symbol of (6^6) and $(4^8{\cdot}5^4{\cdot}6^3)$, respectively. Parallel experiments showed that different Ln cations may lead to the structural distinctions of the resulting products, which can be explained as the influence of the radius of Ln^{III} cations that play a crucial role in the dimensionality of the yielded products. Similar phenomena also can be encountered in the previously reports.[12a] In addition, notice that the $[\alpha\text{-}SiW_{12}O_{40}]^{4-}$ as a starting material was introduced to prepare **1**−**9**, but all the products contain the $[\alpha\text{-}SiW_{11}O_{39}]^{8-}$ anions. When $[\alpha\text{-}SiW_{11}O_{39}]^{8-}$ as the precursor replaced $[\alpha\text{-}SiW_{12}O_{40}]^{4-}$ under the same conditions, we failed, which may be related to the nature of distinct Keggin-type POM precursors and suggests that the transformation from $[\alpha\text{-}SiW_{12}O_{40}]^{4-}$ to $[\alpha\text{-}SiW_{11}O_{39}]^{8-}$ is necessary in the formation of **1**−**9**.

Structural Descriptions. The experimental XRPD patterns for **1**−**9** are in good agreement with the simulated XRPD patterns from the single-crystal X-ray diffraction, demonstrating the good phase purity for **1**−**9** (Figure S1 in the Supporting Information). The differences in intensity between the experimental and simulated XRPD patterns might be due to the variation in preferred orientation of the powder sample during collection of the experimental XRPD. In addition, the bond-valence sum calculations[20] indicate that all W atoms, Cu atoms, and Ln atoms in **1**−**9** are in the +6, +2, and +3 oxidation states, respectively. Considering the charge balance of **1**−**9**, some protons need to be added. To locate the positions of these protons, the bond valence sum calculations of all the oxygen atoms on POM fragments are carried out (Figures S2−S4 and Tables S1−S3 in the Supporting Information). The Ln−O bond lengths (Table S4 in the Supporting Information) decrease as the ionic radius of the Ln^{III} cations decrease, which is in accordance with the effect of the lanthanide contraction.[6,21]

The structural analysis reveals that **1**−**5** are isomorphous and crystallize in the monoclinic space group $P2(1)/c$, thus; only $K(enH_2)_4[Cu(en)_2(H_2O)]_2\{[Cu(en)_2]_{1.5}Gd[(\alpha\text{-}H_{1.75}SiW_{11}O_{39})_2]\}_2\cdot\sim 15H_2O$ (**1**) is taken as an example to describe here. The structural unit of **1** consists of a dimer $\{[Cu(en)_2]_{1.5}Gd[(\alpha\text{-}H_{1.75}SiW_{11}O_{39})_2]\}_2^{13-}$ anion (Figure 1a), four protoned $[enH_2]^{2+}$ ions, two free $[Cu(en)_2(H_2O)]^{2+}$ ions, a K^+ ion, and 15 lattice water molecules. Three independent copper ions exhibit two types of coordination geometries. The $[Cu1(en)_2]^{2+}$ ion exhibits the octahedral geometry with four nitrogen atoms from en ligands

Table 2. Crystallographic Data and Structure Refinements for 1−9

	1		2		3	
formula	$C_{28}H_{161}Cu_5Gd_2KN_{28}O_{173}Si_4W_{44}$		$C_{28}H_{161}Cu_5Tb_2KN_{28}O_{173}Si_4W_{44}$		$C_{32}H_{167}Cu_5Dy_2KN_{32}O_{168}Si_4W_{44}$	
M_r (g mol^{-1})	12531.79		12535.13		12572.42	
space group	$P2(1)/c$		$P2(1)/c$		$P2(1)/c$	
crystal system	monoclinic		monoclinic		monoclinic	
a (Å)	17.545(3)		17.569(3)		17.5614(14)	
b (Å)	24.189(4)		24.235(4)		24.208(2)	
c (Å)	24.659(4)		24.673(4)		24.557(2)	
β (°)	104.053(3)		103.939(4)		104.1320(10)	
V (Å^3)	10152(3)		10196(3)		10123.9(14)	
Z	2		2		2	
crystal size [mm^3]	0.17 × 0.13 × 0.08		0.42 × 0.32 × 0.20		0.31 × 0.23 × 0.15	
D_c (g cm^{-3})	4.095		4.078		4.119	
μ (mm^{-1})	26.118		26.049		26.273	
R_{int}	0.0670		0.0684		0.0935	
reflns collected	51666		47467		51139	
indep reflns	17812		17758		17767	
params	1343		1343		1269	
GOF on F^2	0.989		1.007		1.032	
R_1[a], wR_2[b] [$I > 2\sigma(I)$]	0.0425	0.0723	0.0430	0.0973	0.0615	0.0926
R_1[a], wR_2[b] [all data]	0.0479	0.0762	0.0692	0.1051	0.0690	0.1010
	4		**5**		**6**	
formula	$C_{28}H_{161}Cu_5Er_2KN_{28}O_{173}Si_4W_{44}$		$C_{28}H_{161}Cu_5Lu_2KN_{28}O_{173}Si_4W_{44}$		$C_7H_{36}Cu_{1.5}LaN_7O_{42}SiW_{11}$	
M_r (g mol^{-1})	12551.81		12567.23		3175.07	
space group	$P2(1)/c$		$P2(1)/c$		$P2(1)/n$	
crystal system	monoclinic		monoclinic		monoclinic	
a (Å)	17.5312(16)		17.510(3)		16.6434(9)	
b (Å)	24.212(2)		24.175(4)		13.6944(7)	
c (Å)	24.750(2)		24.658(4)		21.8679(11)	
β (°)	103.919(2)		103.817(3)		107.0910(10)	
V (Å^3)	10196.8(6)		10136(3)		4764.1(4)	
Z	2		2		4	
crystal size [mm^3]	0.18 × 0.14 × 0.12		0.24 × 0.17 × 0.15		0.26 × 0.21 × 0.14	
D_c (g cm^{-3})	4.083		4.113		4.424	
μ (mm^{-1})	26.176		26.480		28.101	
R_{int}	0.0527		0.0692		0.0496	
reflns collected	51534		50922		24151	
indep reflns	17887		17769		8377	
params	1349		1343		655	
GOF on F^2	1.016		1.003		1.022	
R_1[a], wR_2[b] [$I > 2\sigma(I)$]	0.0349	0.0755	0.0413	0.0933	0.0351	0.0737
R_1[a], wR_2[b] [all data]	0.0567	0.0813	0.0635	0.1008	0.0485	0.0776
	7		**8**		**9**	
formula	$C_7H_{34}CeCu_{1.5}N_7O_{41}SiW_{11}$		$C_{16}H_{85}Cu_3N_{16}PrO_{85}Si_2W_{22}$		$C_{18}H_{91}Cu_4N_{18}SmO_{85}Si_2W_{22}$	
M_r (g mol^{-1})	3158.27		6294.34		6425.18	
space group	$P2(1)/n$		$P2(1)/n$		$P2(1)/n$	
crystal system	monoclinic		monoclinic		monoclinic	
a (Å)	16.6217(12)		21.816(12)		22.2470(7)	
b (Å)	13.6670(10)		11.667(7)		11.7997(4)	
c (Å)	21.8926(15)		39.20(2)		39.9452(13)	
β (°)	106.9950(10)		101.698(10)		102.2010(10)	
V (Å^3)	4756.1(6)		9771(10)		10249.1(6)	
Z	4		4		4	
crystal size [mm^3]	0.25 × 0.17 × 0.11		0.28 × 0.25 × 0.21		0.22 × 0.17 × 0.14	
D_c (g cm^{-3})	4.408		4.273		4.093	
μ (mm^{-1})	28.204		27.042		26.078	
R_{int}	0.0479		0.0531		0.0607	
reflns collected	23964		39705		51976	
indep reflns	8353		16849		17946	
params	643		1238		1279	
GOF on F^2	1.049		1.042		1.032	

dx.doi.org/10.1021/cg2012759 | Cryst. Growth Des. 2012, 12, 1263−1272

Table 2. continued

	7		8		9	
R_1[a], wR_2[b] [$I > 2\sigma(I)$]	0.0372	0.0819	0.0455	0.0920	0.0437	0.0971
R_1[a], wR_2[b] [all data]	0.0561	0.0871	0.0680	0.0992	0.0651	0.1042

Scheme 2. Formation Conditions of 1−9

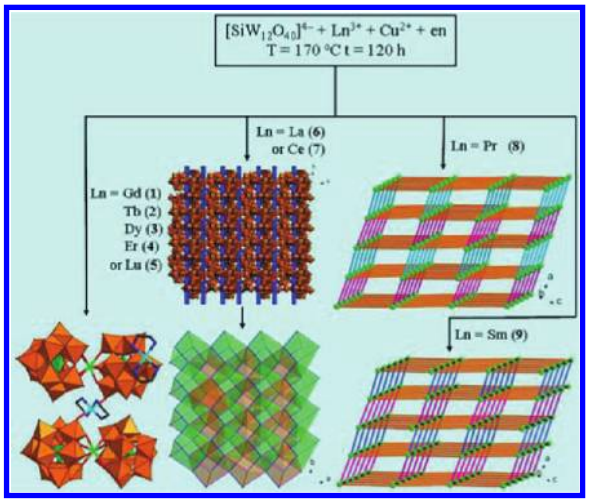

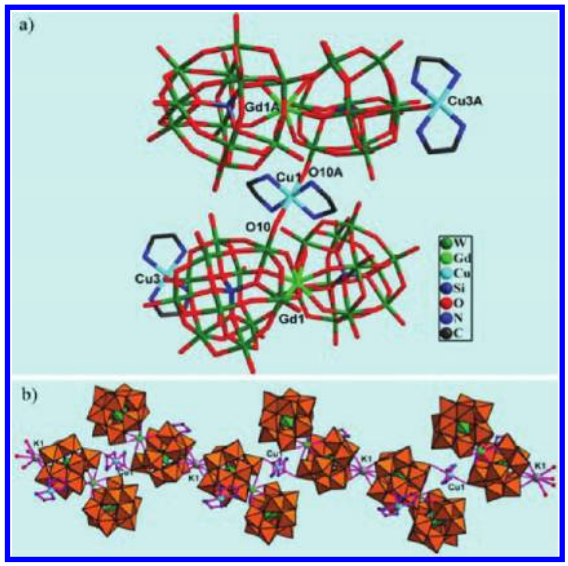

Figure 1. (a) Wire representation of the dimeric structure unit of **1**. (b) The 1D chain built by alternate $[Cu2(en)_2]^{2+}$ bridges and K^+ ions structure of **1**. H atoms, lattice water molecules, free $[Cu2(en)_2(H_2O)]^{2+}$, and protoned $[enH_2]^{2+}$ are omitted for clarity. The atoms with the suffix A is generated by the symmetry operation: $-x$, $1 - y$, $2 - z$.

[Cu−N: 1.968(13)−1.982(13) Å] and two terminal oxygen atoms from the $[Gd(\alpha\text{-}H_{1.75}Si\,W_{11}O_{39})_2]^{9.5-}$ anion [Cu−O: 2.909(12) Å]. The free $[Cu2\ (en)_2(H_2O)]^{2+}$ ion adopts the square pyramid geometry with four nitrogen atoms from two en ligands [Cu−N: 1.965(15)−2.008(17) Å] and one water ligand [Cu−O: 2.526(12) Å]. The $[Cu3(en)_2]^{2+}$ ion displays the same geometry to the $[Cu2(en)_2(H_2O)]^{2+}$, which is defined by four nitrogen atoms from the chelating en ligands [Cu−N: 1.952(17)−2.018(18) Å] and terminal oxygen atom from the $[Gd(\alpha\text{-}H_{1.75}SiW_{11}O_{39})_2]^{9.5-}$ anion [Cu−O: 2.534(12) Å]. The $[Gd(\alpha\text{-}H_{1.75}SiW_{11}O_{39})_2]^{9.5-}$ moiety is constructed from an eight-coordinate Gd^{III} cation sandwiched by two monovacant $[\alpha\text{-}H_{1.75}SiW_{11}O_{39}]^{6.25-}$ units, resulting in a well-known sandwich-type bis(undecatungstophospate) lanthanate structure, which was first discovered by Peacock and Weakley in 1971,[3a] and this 1:2 structural series made up of one Ln cation and two monovacant Keggin-type POM units have been widely investigated.[3c,f] The adjacent $[Gd(\alpha\text{-}H_{1.75}SiW_{11}O_{39})_2]^{9.5-}$ subunits are interconnected by bridging O10−Cu1−O10 connector resulting in the dimer, which represents the first dimer built by 3d-4f heterometals and $[\alpha\text{-}SiW_{11}O_{39}]^{8-}$ subunits. More interestingly, the dimers are connected by K^+ ions forming a novel 1D zigzag chain structure (Figure 1b). In the $[Gd(\alpha\text{-}H_{1.75}SiW_{11}O_{39})_2]^{9.5-}$ sunbunit, the Gd^{III} cation incorporated to the monovacant site of the $[\alpha\text{-}H_{1.75}\ SiW_{11}O_{39}]^{6.25-}$ subunit in the "cap" region, adopting a distorted square antiprismatic coordination geometry (Figure S5a in the Supporting Information), bonding to eight oxygen atoms (O12, O13, O17, O27, O51, O56, O69, O70) from the monovacant sites of two adjacent $[\alpha\text{-}H_{1.75}SiW_{11}O_{39}]^{6.25-}$ units with Gd−O distances of 2.363(10)−2.440(11) Å, and the average of 2.390 Å. In the coordination polyhedron around the Gd^{III} cation, O12, O13, O17, O27 group and O51, O56, O69, O70 group constitute two bottom planes of the square antiprism, and their standard deviations from their least-squares are 0.012 and 0.018 Å, respectively. The dihedral angle for the two bottom surfaces is 1.2°. The distances of the Gd^{III} cation and two bottom surfaces are 1.251 and 1.282 Å, respectively. The above-mentioned data indicate that the square antiprism is somewhat distorted.

X-ray crystallographic analysis reveals that **6**−**7** are isomorphous and crystallize in the monoclinic space group $P2(1)/n$; therefore, only $(enH_2)_{0.5}\{[Cu(en)_2]_{1.5}La[(\alpha\text{-}HSiW_{11}O_{39})]\}\cdot\sim 3H_2O$ (**6**) is discussed in detail. The structural unit of **6** consists of a 1:1 type of $\{[Cu(en)_2]_{1.5}\ La[(\alpha\text{-}HSiW_{11}O_{39})]\}^-$ anion (Figure 2a), a half protoned $[enH_2]^{2+}$ ion, and three lattice water molecules. Two crystallographic unique copper ions Cu1 and Cu2 exhibit the same octahedral geometries. It is worth noting that the square antiprism coordination sphere of the La^{III} cations in the vacant site of the lacunary $[\alpha\text{-}HSiW_{11}O_{39}]^{7-}$ units are completed by four μ_2-O and four μ_3-O atoms from two neighboring $[\alpha\text{-}HSiW_{11}O_{39}]^{7-}$ units, which are different from the previous reports.[3b,12a] This coordination mode of La cations has not been discovered in POM chemistry (Figure S5b in the Supporting Information). The $[\alpha\text{-}HSiW_{11}O_{39}]^{7-}$ units are connected by the La^{III} cations forming a 1D helical chainlike structure (Figure 2b). Such an arrangement can be comparable to those found in the 1D homometallic lanthanide substituted POMs $[Ln(\alpha\text{-}SiW_{11}O_{39})(H_2O)_3]^{5-}$ (Ln = La^{III}, Ce^{III}) (**A**)[3b] and 3d-4f heterometallic POMs $[(Cu(en)(OH))_3]Ln[(SiW_{11}O_{39})(H_2O)]^{2-}$.[12a] In comparison with **A**,[3b] some obvious distinctions are observed in **6**: (a) **6** was synthesized under hydrothermal conditions other than the conventional aqueous solution; (b) **6** was prepared by reaction of the saturated Keggin $[SiW_{12}O_{40}]^{4-}$anions, while **A**[3b] were all isolated by the monovacant Keggin $[SiW_{11}O_{39}]^{8-}$ subunits; (c) the La cations in **6** are coordinated by eight oxygen atoms from two adjacent $[\alpha\text{-}SiW_{11}O_{39}]^{8-}$ subunits, whereas the Ln cations in **A** are coordinated by nine oxygen atoms in a distorted monocapped square antiprism.[3b] (d) **6** is the 3D framework (Figure 2c), on the contrary, **A** displays the 1D helical chain. From the topological point of view, if each $\{La[(\alpha\text{-}HSiW_{11}O_{39})]\}^{4-}$ subunit acts as a 5-connected node, the 3D framework of **6** can be described as a 5-connected network

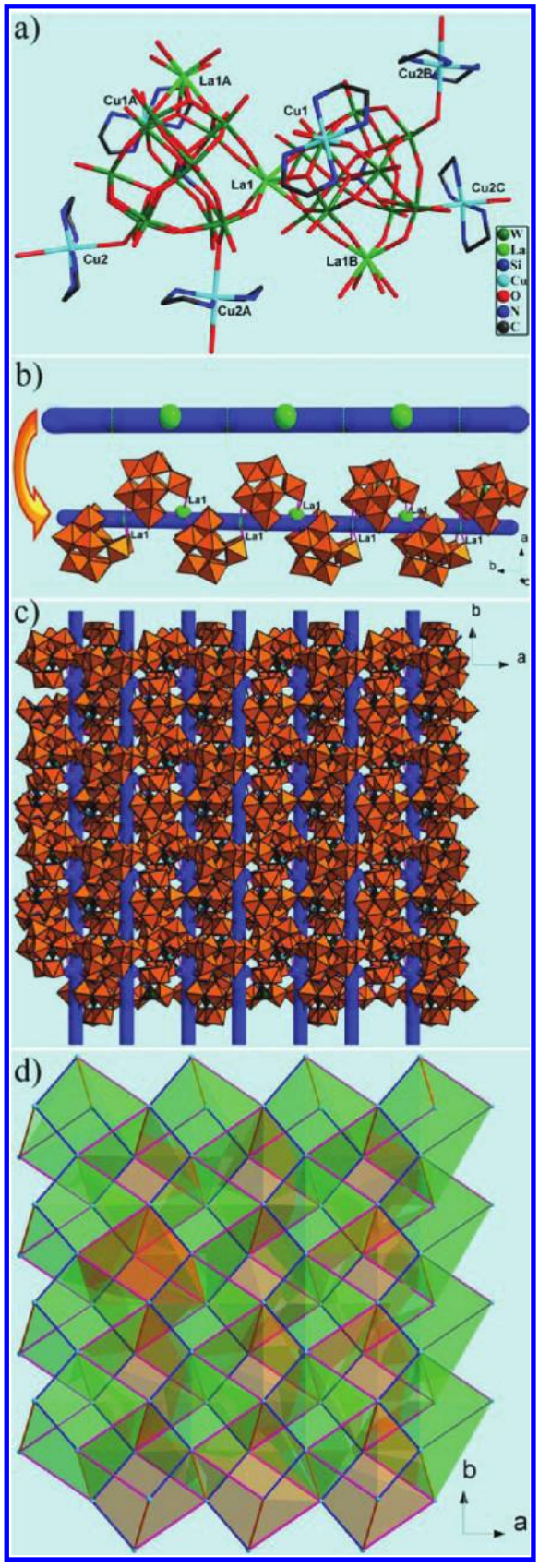

Figure 2. (a) Wire representation of the molecular structural unit of **6**. (b) The 1D helical chain built by La^{III} cations and $[\alpha\text{-}SiW_{11}O_{39}]^{8-}$ ions. (c) The 3D framework of **6**. (d) The $(4^8{\cdot}6^2)$ topology network. H atoms, lattice water molecules, and protoned $[enH_2]^{2+}$ are omitted for clarity. The atoms with the suffixes A, B, C are generated by the symmetry operation: 1.5 − *x*, 0.5 + *y*, 0.5 − *z*; 1.5 − *x*, −0.5 + *y*, 0.5 − *z*; 1 + *x*, −1 + *y*, *z*, respectively.

with the Schläfli symbol of $(4^8{\cdot}6^2)$ (Figure 2d), which is distinguished from the 5-connected $(4^8{\cdot}6^2)$ topology structure in our previous report.[13c] Though some 5-connected uninodal nets have been described, this 5-connected uninodal net has not been discovered in the domain of POM chemistry. As far as we know, only one example of organic−inorganic hybrid 3d-4f heteromatellic 2D silicotungstate $[(Cu(en)(OH))_3]$ $La[(SiW_{11}O_{39})]^{2-}$ (**B**) was obtained by Mialane et al.[12a] Notably, the construction mode of the 3D structure in **6** is different from that in **B**.[12a] Compared with **B**,[12a] two common features are found: (a) Both **B**[12a] and **6** were obtained by hydrothermal treatment, which further corroborates that the hydrothermal method is an effective strategy in giving novel organic−inorganic hybrid POM derivatives; (b) both contain the $[\alpha\text{-}SiW_{11}O_{39}]^{8-}$ units, 3d-4f heterometals and $[Cu(en)_2]^{2+}$ ions. The major discrepancies are as follows: (a) **B**[12a] was prepared by trivacant Keggin precursor $[\alpha\text{-}SiW_9O_{34}]^{10-}$ units, whereas **6** was synthesized by the saturated Keggin $[\alpha\text{-}SiW_{12}O_{40}]^{4-}$; (b) The La cations in **B**[11a] are linked by five μ_2-O, two μ_3-OH ligands and a terminal μ_3-O atom, while the La cations in **6** are connected four μ_2-O and four μ_3-O atoms from two neighboring $[\alpha\text{-}SiW_{11}O_{39}]^{8-}$ subunits; (c) above all, each La cation in **B**[12a] occupies the vacant site of the monovacant $[\alpha\text{-}SiW_{11}O_{39}]^{8-}$ unit and is linked to three $\{Cu^{II}(en)\}$ groups via two μ_3-OH ligands and a terminal μ_3-O atom of the $[\alpha\text{-}SiW_{11}O_{39}]^{8-}$ subunit ligand, producting a distorted $\{LnCu_3(OH)_3O\}$ cubane fragment, which does not exist in **6**.

In the case of **8**−**9**, they are isomorphous and all belong to the monoclinic space group *P*2(1)/*n*. Hence, only $(enH_2)_2\{[Cu(en)_2(H_2O)][Cu(en)_2]_2Pr[(\alpha\text{-}H_{1.5}SiW_{11}O_{39})_2]\}{\cdot}{\sim}6H_2O$ (**8**) is represented herein. The structural unit of **8** consists of one $\{[Cu(en)_2(H_2O)][Cu(en)_2]_2Pr[(\alpha\text{-}H_{1.5}SiW_{11}O_{39})_2]\}^{4-}$ subunit (Figure 3a), two protoned $[enH_2]^{2+}$ ions, and six lattice water molecules. Four crystallographic unique copper cations are in the distorted octahedral geometry. The Pr^{III} cation is coordinated by two neighboring $[\alpha\text{-}H_{1.5}SiW_{11}O_{39}]^{6.5-}$ anions, through eight vacant oxygen atoms in a distorted square antiprismatic geometry (Figure S5c in the Supporting Information). Alternatively, **8** can also be viewed as the same dimer to **1** except that the bridging O10−Cu1−O10 is replaced by $[Cu3(en)_2]^{2+}$ and $[Cu4(en)_2]^{2+}$ groups; in contrast, in **8**, adjacent $[Pr(\alpha\text{-}H_{1.5}SiW_{11}O_{39})_2]^{10-}$ anions are linked together by alternate $[Cu3(en)_2]^{2+}$ and $[Cu4\ (en)_2]^{2+}$ ions generating the 1D zigzag chain along the *b* axis. The most remarkable of **8** is that each $[Pr(\alpha\text{-}H_{1.5}SiW_{11}O_{39})_2]^{10-}$ subunit acts as a penta-dentate ligand to join five $[Cu(en)_2]^{2+}$ groups leading to a fascinating 3D framework, which is the first organic−inorganic hybrid 3D 3d-4f heterometallic silicotungstate (Figure 3b). From the topological point of view, the circuit symbols Schläfli (vertex) notations can be used to describe topologies and facilitate comparison of networks of different composition and metrics.[22] If each $\{[Cu(en)_2(H_2O)][Cu(en)_2]_2Pr[(\alpha\text{-}H_{1.5}SiW_{11}O_{39})_2]\}^{4-}$ subunit is viewed as a 4-connected node, the 3D framework of **8** is a 4-connected 3D network with the Schläfli symbol of (6^6) (Figure 3c), which is different from the known 4-connected topologies of minerals such as NbO $(6_2{\cdot}6_2{\cdot}6_2{\cdot}6_2{\cdot}8_2{\cdot}8_2)$, quartz $(6{\cdot}6{\cdot}6_2{\cdot}6_2{\cdot}8_7{\cdot}8_7)$, sodalite $(4{\cdot}4{\cdot}6{\cdot}6{\cdot}6{\cdot}6)$, $CdSO_4$ $(6{\cdot}6{\cdot}6{\cdot}6{\cdot}6_2{\cdot}{*})$, CrB_4 $(4{\cdot}6_2{\cdot}6{\cdot}6{\cdot}6{\cdot}6)$, moganite $(4{\cdot}4{\cdot}6_2{\cdot}6_2{\cdot}\ 8_4{\cdot}8_4)$ and PtS $(4{\cdot}4{\cdot}8_2{\cdot}8_2{\cdot}8_2{\cdot}8_2)$.[23]

Topological analysis of **8** and **9** by examining the schematic representations of their chemical connectivity facilitates the description and comparison of two different 3D architectures, though **8** and **9** are isomorphous and both exhibit the rare 3D 3d-4f heterometallic silicotungstates. **8** exhibits the 3D topology with the Schläfli notation (6^6), whereas **9** shows the Schläfli notation $(4^8{\cdot}5^4{\cdot}6^3)$. In **9**, four of five crystallographic unique

dx.doi.org/10.1021/cg2012759 | *Cryst. Growth Des.* 2012, 12, 1263−1272

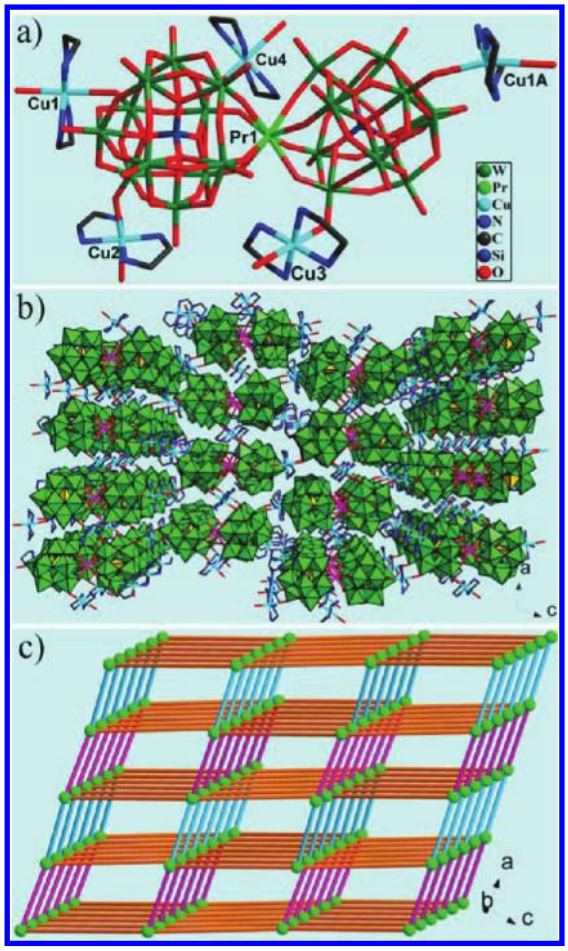

Figure 3. (a) Wire representation of the molecular structural unit of **8**. (b) The 3D framework structure showing the −ABAB− mode. (c) The (6^6) topology framework of **8**. H atoms, lattice water molecules, and protoned $[enH_2]^{2+}$ are omitted for clarity. The atoms with the suffix A is generated by the symmetry operation: 0.5 + *x*, 3.5 − *y*, 0.5 + *z*.

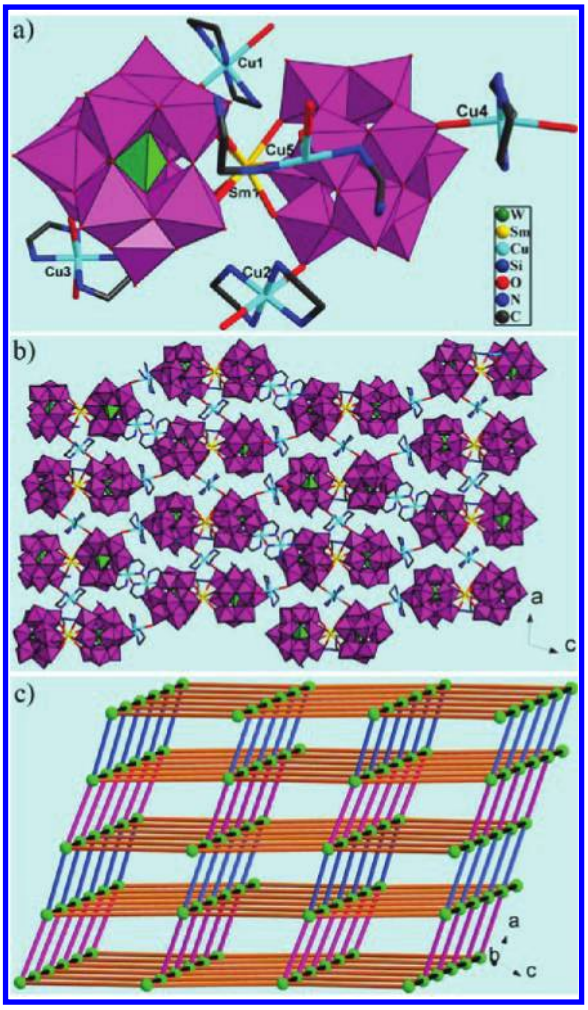

Figure 4. (a) Wire/polyhedral representation of the molecular structural unit of **9**. (b) The 3D framework structure showing the −ABAB− mode. (c) The ($4^8.5^4.6^3$) topology framework of **9**. H atoms, lattice water molecules, and protoned $[enH_2]^{2+}$ are omitted for clarity.

copper cations are in the distorted octahedral geometry except that the $[Cu5(Hen)_2]^{4+}$ ion forms a distorted square geometry defined by two terminal oxygen atoms from the adjacent $[Sm(\alpha\text{-}SiW_{11}O_{39})_2]^{13-}$ anions [Cu−O: 2.860(8) and 2.311(9)Å]. In the $[Cu5(Hen)_2]^{4+}$ ion, two monoprotonated $[Hen]^+$ ligands in an uncommon end-on coordination motif [Cu−N: 1.927(19) and 1.980(16)Å] (Figure 4a), which is very similar to the coordination motif of the N_3^- ligand in $[\{(\gamma\text{-}SiW_{10}O_{36})\ Mn_2(OH)_2(N_3)_{0.5}(H_2O)_{0.5}\}_2(\mu\text{-}1,3\text{-}N_3)]^{10-}$.[24] Such end-on coordination motif of en is very rare in POM chemistry.[25] The most intriguing beautiful feature of **9** is that each $[Sm(\alpha\text{-}SiW_{11}O_{39})_2]^{13-}$ subunit acts as a heptadentate ligand to connect seven $[Cu(en)_2]^{2+}$ groups generating a fascinating 6-connected 3D framework (Figure 4b), which still represents the first 3D framework with the Schläfli notation ($4^8.5^4.6^3$) in POM chemistry (Figure 4c), being similar to those oberved in a previous **pcu** ($4^{12}.6^3$) net but display very rare ($4^8.5^4.6^3$) net topology.[26] To the best of our knowledge, this six-connected uninodal net has not been described in the domain of POM chemistry and has only been encountered in a couple of hydrogen-bonded nets and two examples of the metal−organic frameworks.[26]

Photoluminescence Properties. Considering the excellent luminescent behaviors of Ln cations,[27] the solid-state excitation and emission spectra of **2**, **3**, and **9** were discussed at ambient temperature, respectively. The excitation spectrum of **2** shows characteristic peaks of Tb^{III} between 250 and 400 nm with a maximum at around 298 nm (Figure S6a). The emission spectrum of **2** at the excited wavelength of 298 nm yields the evident emission peaks $^5D_4 \rightarrow {}^7F_J$ (J = 6, 5, 4, and 3) of Tb^{III} ion,[27d,e] which are assigned to $^5D_4 \rightarrow {}^7F_6$ (492 nm), $^5D_4 \rightarrow {}^7F_5$ (547 nm), $^5D_4 \rightarrow {}^7F_4$(594 nm), and $^5D_4 \rightarrow {}^7F_3$ (622 nm) transitions, respectively (Figure 5a). Moreover, the emission band at 547 nm attributable to the $^5D_4 \rightarrow {}^7F_5$ transition is the strongest, which is comparable with the previous observation in

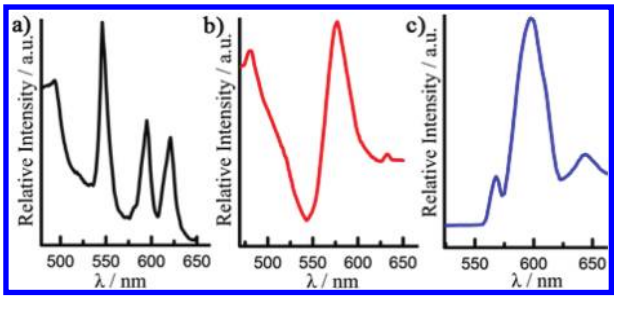

Figure 5. The solid-state emission spectra of **2** (a), **3** (b), and **9** (c) at room temperature. The emission spectra were recorded at λ_{ex} = 298 nm for **2**, λ_{ex} = 356 nm for **3**, and λ_{ex} = 377 nm for **9**, respectively.

dx.doi.org/10.1021/cg2012759 | *Cryst. Growth Des.* 2012, 12, 1263−1272

Tb^{III}-containing compounds.[27d,e] The excitation spectrum of **3** consists of two bands at around 356 and 381 nm (Figure S6b). Excitation of the as-synthesized solid of **3** at 356 nm reveals the typical Dy^{III} emissions at 481, 577, and 632 nm (Figure 5b), originating from the characteristic emission $^4F_{9/2} \rightarrow {}^6H_J$ (J = 15/2, 13/2, and 11/2) transitions of the Dy^{III} cation, respectively.[27f] In addition, the emission wavelength of at 577 nm is the most intense, being in agreement with the previous results of Dy^{III} cations.[27f] Meantime, it is obvious that the intensity of the yellow emission corresponding to $^4F_{9/2} \rightarrow {}^6H_{13/2}$ transition is stronger than the blue emission of the $^4F_{9/2} \rightarrow {}^6H_{15/2}$ transition, indicating that the $[\alpha\text{-}SiW_{11}O_{39}]^{8-}$ ligands may be suitable for the sensitization of the yellow luminescence for Dy^{III} cations.[27f] In the case of **9**, the excitation spectrum reveals a wide band between 350 and 450 nm with a maximum at 377 nm (Figure S6c). Compound **9** exhibits the characteristic transitions of Sm^{III} ions upon excitation at 377 nm. As shown in Figure 5c, transitions from the excited $^4G_{5/2}$ state to the different J levels of the lower ^6H_J (J = 5/2, 7/2, and 9/2) state were observed in the emission spectrum, that is, $^4G_{5/2} \rightarrow {}^6H_{5/2}$ at 567 nm, $^4G_{5/2} \rightarrow {}^6H_{7/2}$ at 597 nm, and $^4G_{5/2} \rightarrow {}^6H_{9/2}$ at 643 nm.[27e] And the most intense peak is the transition $^4G_{5/2} \rightarrow {}^6H_{7/2}$ at 597 nm, being in good accordance with the previous reports.[27e] In order to determine the fluorescence signals originating from POM ligand-to-metal charge transfer (LMCT) bands or the f-f transitions of the Ln cations, the photochemistry of $K_8[(\alpha\text{-}SiW_{11}O_{39})]$ has also been measured (Figure S7). Two emission bands at 467 and 491 nm assigned to $^3T_{1u} \rightarrow {}^1A_{1g}$ transitions deriving from the O → W LMCT transitions of silicotungstates can be detected,[28] which is in accordance with the established work by Yamase et al., who have shown that the intramolecular energy transfer from the O → M LMCT excited states to the Ln cations can occur in the POM system.[27a,b] This phenomenon has been observed in the sensitized luminescence Eu^{III}, Mn^{IV}, Cr^{III}, and Cd^{II} POMs as a result of intramolecular energy transfer.[27b,28] Compared Figure 5 with Figure S7, it can be seen that the fluorescence signals of **2**, **3**, and **9** mainly originate from the f-f transitions of the Ln cations.

CONCLUSIONS

In conclusion, a family of novel organic−inorganic hybrid lacunary Keggin silicotungstate 3d-4f heterometallic derivatives **1**−**9** have been hydrothermally synthesized and structurally characterized. **1**−**5** exhibit the dimeric structures; **6**−**9** all display the unprecedented 3D frameworks, but with three different Schläfli symbols of $(4^8{\cdot}6^2)$, $(4^8{\cdot}6^2)$, (6^6) and $(4^8{\cdot}5^4{\cdot}6^3)$, respectively, representing the first 3D 3d-4f heterometallic silicotungstates. Furthermore, the luminescence properties of **2**, **3**, and **9** have been investigated. The successful isolations of **1**−**9** suggest that self-assembly of POMs, Ln salts, TM salts, and organic ligands in a one-pot hydrothermal reaction is an effective strategy in constructing 3d-4f heterometallic POM hybrids. Actually, the combination of heterometallic complex precursors with POM components and incorporation of 4f cations to 3d-substituted POMs have developed as two other strategies to preparing 3d-4f heterometallic POMs:[4−13] As a result, to obtain many more 3d-4f heterometallic POMs with unexpected structures and properties, lots of work needs to be done by synthetic chemists.

ASSOCIATED CONTENT

Supporting Information

Representations of XPRD patterns, discussion on the location of protons, the Ln−O bond lengths, the coordination environments of the Ln cations, IR spectra, TG analyses, and X-ray crystallographic data of **1**−**9** in CIF format. This material is available free of charge via the Internet at http://pubs.acs.org.

AUTHOR INFORMATION

Corresponding Author

*Fax: (+86) 378 3886876. E-mail: jpwang@henu.edu.cn (J.W.), jyniu@henu.edu.cn (J.N.).

ACKNOWLEDGMENTS

This work was supported by the Natural Science Foundation of China, Special Research Fund for the Doctoral Program of Higher Education, Innovation Scientists and Technicians Troop Construction Projects of Henan Province and Natural Science Foundation of Henan Province.

REFERENCES

(1) (a) Streb, C.; Ritchie, C.; Long, D. L.; Kögerler, P.; Cronin, L. *Angew. Chem., Int. Ed.* **2007**, *46*, 7579−7582. (b) Mitchell, S. G.; Streb, C.; Miras, H. N.; Boyd, T.; Long, D. L.; Cronin, L. *Nat. Chem.* **2010**, *2*, 308−312. (c) Besson, C.; Huang, Z. Q.; Geletii, Y. V.; Lense, I.; Hardcastle, S. K.; Musaev, D. G.; Lian, T. Q.; Anna, P.; Hill, C. L. *Chem. Commun.* **2009**, 2784−2786. (d) Long, D. L.; Tsunashima, R.; Cronin, L. *Angew. Chem., Int. Ed.* **2010**, *49*, 1736−1758. (e) Song, Y. F.; Long, D. L.; Cronin, L. *Angew. Chem., Int. Ed.* **2007**, *46*, 3900−3904. (f) Sartorel, A.; Carraro, M.; Scorrano, G.; De Zorzi, R.; Geremia, S.; McDaniel, N. D.; Bernhard, S.; Bonchio, M. *J. Am. Chem. Soc.* **2008**, *130*, 5006−5007. (g) Sun, C. Y.; Liu, S. X.; Liang, D. D.; Shao, K. Z.; Ren, Y. H.; Su, Z. M. *J. Am. Chem. Soc.* **2009**, *131*, 1883−1888. (h) Jiang, C. J.; Lesbani, A.; Kawamoto, R.; Uchida, S.; Mizuno, N. *J. Am. Chem. Soc.* **2006**, *128*, 14240−14241. (i) Ritchie, C.; Streb, C.; Thiel, J.; Mitchell, S. G.; Miras, H. N.; Long, D. L.; Boyd, T.; Peacock, R. D.; McGlone, T.; Cronin, L. *Angew. Chem., Int. Ed.* **2007**, *46*, 7579−7582.

(2) (a) Felices, L. S.; Vitoria, P.; Gutiérrez Zorrilla, J. M.; Lezama, L.; Reinoso, S. *Inorg. Chem.* **2006**, *45*, 7748−7757. (b) Katsoulis, D. E.; Pope, M. T. *J. Am. Chem. Soc.* **1984**, *106*, 2737−2738. (c) Lahootun, V.; Besson, C.; Villanneau, R.; Villain, F.; Chamoreau, L M.; Boubekeur, K.; Blanchard, S.; Thouvenot, R.; Proust, A. *J. Am. Chem. Soc.* **2007**, *129*, 7127−7135. (d) Felices, L. S.; Vitoria, P.; Gutiérrez Zorrilla, J. M.; Reinoso, S.; Etxebarria, J.; Lezama, L. *Chem.—Eur. J.* **2004**, *10*, 5138−5146. (e) Hussain, F.; Bassil, B. S.; Bi, L. H.; Reicke, M.; Kortz, U. *Angew. Chem., Int. Ed.* **2004**, *43*, 3485−3488. (f) Mialane, P.; Dolbecq, A.; Marrot, J.; Rivière, E.; Sécheresse, F. *Chem.—Eur. J.* **2005**, *11*, 1771−1778. (g) Zheng, S. T.; Yuan, D. Q.; Jia, H. P.; Zhang, J.; Yang, G. Y. *Chem. Commun.* **2007**, 1858−1860.

(3) (a) Peacock, R. D.; Weakley, T. J. R. *J. Chem. Soc. A.* **1971**, 1836−1839. (b) Sadakane, M.; Dickman, M. H.; Pope, M. T. *Angew. Chem., Int. Ed. Engl.* **2000**, *39*, 2914−2916. (c) Mialane, P.; Lisnard, L.; Mallard, A.; Marrot, J.; Antic Fidancev, E.; Aschehoug, P.; Vivien, D.; Sécheresse, F. *Inorg. Chem.* **2003**, *42*, 2102−2108. (d) Mialane, P.; Dolbecq, A.; Rivière, E.; Marrot, J.; Sécheresse, F. *Eur. J. Inorg. Chem.* **2004**, 33−36. (e) Kholdeeva, O. A.; Timofeeva, M. N.; Maksimov, G. M.; Maksimovskaya, R. I.; Neiwert, W. A.; Hill, C. L. *Inorg. Chem.* **2005**, *44*, 666−672. (f) Bassil, B. S.; Dickman, M. H.; von der Kammer, B.; Kortz, U. *Inorg. Chem.* **2007**, *46*, 2452−2458.

(4) (a) Reinoso, S. *Dalton Trans.* **2011**, *40*, 6610−6615. (b) Yao, S.; Zhang, Z. M.; Li, Y. G.; Lu, Y.; Wang, E. B.; Su, Z. M. *Cryst. Growth Des.* **2010**, *10*, 135−139. (c) Li, Y. W.; Li, Y. G.; Wang, Y. H.; Feng, X. J.; Lu, Y.; Wang, E. B. *Inorg. Chem.* **2009**, *48*, 6452−6458. (d) Fang, X. K.; Kögerler, P. *Angew. Chem., Int. Ed.* **2008**, *47*, 8123−8126. (e) Fang, X. K.; Kögerler, P. *Chem. Commun.* **2008**, 3396−3398.

(5) Merca, A.; Müller, A.; Slageren, J. V.; Läge, M.; Krebs, B. *J. Clust. Sci.* **2007**, *18*, 711−719.

(6) Cao, J. F.; Liu, S. X.; Cao, R. G.; Xie, L. H.; Ren, Y. H.; Gao, C. Y.; Xu, L. *Dalton Trans.* **2008**, 115−120.

(7) Chen, W. L.; Li, Y. G.; Wang, Y. H.; Wang, E. B.; Zhang, Z. M. *Dalton Trans.* **2008**, 865−867.

(8) Reinoso, S.; Galán Mascarós, J. R. *Inorg. Chem.* **2010**, *49*, 377–379.
(9) (a) Li, B.; Zhao, J. W.; Zheng, S. T.; Yang, G. Y. *J. Clust. Sci.* **2009**, *20*, 503–513. (b) Du, D. Y.; Qin, J. S.; Li, S. L.; Wang, X. L.; Yang, G. S.; Li, Y. G.; Shao, K. Z.; Su, Z. M. *Inorg. Chem. Acta.* **2010**, *363*, 3823–3831.
(10) Pang, H. J.; Zhang, C. J.; Shi, D. M.; Chen, Y. G. *Cryst. Growth Des.* **2008**, *8*, 4476–4480.
(11) (a) Chen, W. L.; Li, Y. G.; Wang, Y. H.; Wang, E. B. *Eur. J. Inorg. Chem.* **2007**, 2216–2220. (b) Zhang, Z. M.; Li, Y. G.; Chen, W. L.; Wang, E. B.; Wang, X. L. *Inorg. Chem. Commun.* **2008**, *11*, 879–882. (c) Zhang, Z. M.; Li, Y. G.; Yao, S.; Wang, E. B. *Dalton Trans.* **2011**, 6475–6479.
(12) (a) Nohra, B.; Mialane, P.; Dolbecq, A.; Rivière, E.; Marrot, J.; Sécheresse, F. *Chem. Commun.* **2009**, 2703–2705. (b) Compain, J. D.; Mialane, P.; Dolbecq, A.; Mbomekallé, I. M.; Marrot, J.; Sécheresse, F.; Duboc, C.; Rivière, E. *Inorg. Chem.* **2010**, *49*, 2851–2858.
(13) (a) Wang, J. P.; Yan, Q. X.; Du, X. D.; Niu, J. Y. *J. Clust. Sci.* **2008**, *19*, 491–498. (b) Shi, D. Y.; Chen, L. J.; Zhao, J. W.; Wang, Y.; Ma, P. T.; Niu, J. Y. *Inorg. Chem. Commun.* **2011**, *14*, 324–329. (c) Niu, J. Y.; Zhang, S. W.; Chen, H. N.; Zhao, J. W.; Ma, P. T.; Wang, J. P. *Cryst. Growth Des.* **2011**, *11*, 3769–3777.
(14) (a) Chen, J.; Sha, J. Q.; Peng, J.; Shi, Z. Y.; Tian, A. X.; Zhang, P. P. *J. Mol. Struct.* **2009**, *917*, 10–14. (b) Laronze, N.; Marrot, J.; Hervé, G. *Inorg. Chem.* **2003**, *42*, 5857–5862. (c) Li, M. X.; Du, J.; Wang, J. P.; Niu, J. Y. *Inorg. Chem. Commun.* **2007**, *10*, 1391–1393. (d) Zhang, Z. M.; Wang, E. B.; Li, Y. G.; An, H. Y.; Qi, Y. F.; Xu, L. *J. Mol. Struct.* **2008**, *872*, 176–181. (e) Chen, W. L.; Chen, B. W.; Tan, H. Q.; Li, Y. G.; Wang, Y. H.; Wang, E. B. *J. Solid State Chem.* **2010**, *183*, 310–321. (f) Ritchie, C.; Burkholder, E.; Kögerler, P.; Cronin, L. *Dalton Trans.* **2006**, 1712–1714. (g) Zhao, J. W.; Zheng, S. T.; Yang, G. Y. *J. Solid State Chem.* **2008**, *181*, 2205–2216. (h) Hussain, F.; Bassil, B. S.; Bi, L. H.; Reicke, M.; Kortz, U. *Angew. Chem., Int. Ed.* **2004**, *43*, 3485–3488. (i) Mialane, P.; Dolbecq, A.; Marrot, J.; Rivière, E.; Sécheresse, F. *Chem.—Eur. J.* **2005**, *11*, 1771–1778. (j) Lisnard, L.; Mialane, P.; Dolbecq, A.; Marrot, J.; Clemente-Juan, J. M.; Coronado, E.; Keita, B.; de Oliveira, P.; Nadjo, L.; Sécheresse, F. *Chem.—Eur. J.* **2007**, *13*, 3525–3536. (k) Kikukawa, Y. J.; Yamaguchi, K.; Mizuno, N. *Inorg. Chem.* **2010**, *49*, 8194–8196. (l) Bassil, B. S.; Kortz, U.; Tigan, A. S.; Clemente-Juan, J. M.; Keita, B.; de Oliveira, P.; Nadjo, L. *Inorg. Chem.* **2005**, *44*, 9360–9368. (m) Ritchie, C.; Ferguson, A.; Nojiri, H.; Miras, H. N.; Song, Y. F.; Long, D. L.; Burkholder, E.; Murrie, M.; Kögerler, P.; Brechin, E. K.; Cronin, L. *Angew. Chem., Int. Ed.* **2008**, *47*, 5609–5612. (n) Kortz, U.; Matta, S. *Inorg. Chem.* **2001**, *40*, 815–817.
(15) (a) Zhao, J. W.; Wang, C. M.; Zhang, J.; Zheng, S. T.; Yang, G. Y. *Chem.—Eur. J.* **2008**, *14*, 9223–9239. (b) Zhao, J. W.; Zhang, H. P.; Jia, J.; Zheng, S. T.; Yang, G. Y. *Chem.—Eur. J.* **2007**, *13*, 10030–10045.
(16) Li, B.; Zhao, J. W.; Zheng, S. T.; Yang, G. Y. *Inorg. Chem.* **2009**, *48*, 8294–8303.
(17) Rocchiccioli-Deltcheff, C.; Fournier, M.; Franck, R.; Thouvenot, R. *Inorg. Chem.* **1983**, *22*, 207–216.
(18) (a) Sheldrick, G. M. *SHELXS97, Program for Crystal Structure Solution*; University of Göttingen: Göttingen, Germany, 1997; (b) Sheldrick, G. M. *SHELXL97, Program for Crystal Structure Refinement*; University of Göttingen: Göttingen, Germany, 1997.
(19) (a) Howell, R. C.; Perez, F. G.; Jain, S.; Horrocks, W. D.; Rheingold, A. L.; Francesconi, L. C. *Angew. Chem., Int. Ed.* **2001**, *40*, 4031–4034. (b) Bassil, B. S.; Dickman, M. H.; Römer, I.; Kammer, B.; Kortz, U. *Angew. Chem., Int. Ed.* **2007**, *46*, 6192–6195. (c) Boglio, C.; Micoine, K.; Rémy, P.; Hasenknopf, B.; Thorimbert, S.; Lacôte, E.; Malacria, M.; Afonso, C.; Tabet, J. C. *Chem.—Eur. J.* **2007**, *13*, 5426–5432.
(20) (a) Brown, I. D.; Altermatt, D. *Acta Crystallogr.* **1985**, *B41*, 244–247. (b) Brese, N. E.; O'Keeffe, M. *Acta Crystallogr.* **1991**, *B47*, 192–197. (c) O'Keeffe, M.; Brese, N. E. *Acta Crystallogr.* **1992**, *B48*, 152–154.
(21) (a) López, X.; Bo, C.; Poblet, J. M. *J. Am. Chem. Soc.* **2002**, *124*, 12574–12582. (b) Gautier, R.; Andersen, O. H.; Gougeon, P.; Halet, J. F.; Canadell, E.; Martin, D. D. *Inorg. Chem.* **2002**, *41*, 4689–4699. (c) Gaunt, A. J.; May, I.; Sarsfield, M. J.; Collison, D.; Helliwell, M.; Denniss, I. S. *Dalton Trans.* **2003**, 2767–2771.
(22) Moulton, B.; Abourahma, H.; Bradner, M. W.; Lu, J. J.; McManus, G. J.; Zaworotko, M. J. *Chem. Commun.* **2003**, 1342–1343.
(23) O'Keeffe, M.; Eddaoudi, M.; Li, H.; Reineke, T.; Yaghi, O. M. *J. Solid State Chem.* **2000**, *152*, 3–20.
(24) Mialane, P.; Duboc, C.; Marrot, J.; Rivière, E.; Dolbecq, A.; Sécheresse, F. *Chem.—Eur. J.* **2006**, *12*, 1950–1959.
(25) (a) Zhang, Z. M.; Liu, J.; Wang, E. B.; Qin, C.; Li, Y. G.; Qi, Y. F.; Wang, X. L. *Dalton Trans.* **2008**, 463–468. (b) Ma, P. T.; Chen, L. J.; Zhao, J. W.; Wang, W.; Wang, J. P.; Niu, J. Y. *Inorg. Chem. Commun.* **2011**, *14*, 415–418.
(26) (a) Guo, H. D.; Guo, X. M.; Batten, S. R.; Song, J. F.; Song, S. Y.; Dang, S.; Zheng, G. L.; Tang, J. K.; Zhang, H. J. *Cryst. Growth Des.* **2009**, *9*, 1394–1401. (b) Yan, L.; Yue, Q.; Jia, Q. X.; Lemercier, G.; Gao, E. Q. *Cryst. Growth Des.* **2009**, *9*, 2984–2987. (c) Baburin, I. A.; Blatov, V. A. *Acta Crystallogr.* **2007**, 791–802. (d) Baburin, I. A. *Z. Kristallogr.* **2008**, *223*, 371–381.
(27) (a) Yamase, T. *Handb. Phys. Chem. Rare Earths* **2009**, *39*, 297–354. (b) Yamase, T. *Chem. Rev.* **1998**, *98*, 307–325. (c) Howell, R. C.; Perez, F. G.; Jain, S.; Horrock, W. D. Jr; Rheingold, A. L.; Francesconi, L. C. *Angew. Chem., Int. Ed.* **2001**, *40*, 4031–4034. (d) Ritchie, C.; Moore, E. G.; Speldrich, M.; Kögerler, P.; Boskovic, C. *Angew. Chem., Int. Ed.* **2010**, *49*, 7702–7705. (e) Zhu, Y. Y.; Sun, Z. G.; Chen, H.; Zhang, J.; Zhao, Y.; Zhang, N.; Liu, L.; Lu, X.; Wang, W. N.; Tong, F.; Zhang, L. C. *Cryst. Growth Des.* **2009**, *9*, 3228–3234. (f) Sun, Y. Q.; Zhang, J.; Chen, Y. M.; Yang, G. Y. *Angew. Chem., Int. Ed.* **2005**, *44*, 5814–5817.
(28) Chen, L. J.; Shi, D. Y.; Zhao, J. W.; Wang, Y. L.; Ma, P. T.; Wang, J. P.; Niu, J. Y. *Cryst. Growth Des.* **2011**, *11*, 1913–1923.